EUROPEAN ORGANIZATION FOR NUCLEAR RESEARCH

CERN–PPE/95-114

21 July 1995

A Measurement of the τ Leptonic Branching Fractions

DELPHI Collaboration

Abstract

A sample of 25000 $Z^0 \to \tau^+\tau^-$ events collected by the DELPHI experiment at LEP in 1991 and 1992 is used to measure the leptonic branching fractions of the τ lepton. The results are $B(\tau \to e\nu\bar{\nu}) = (17.51 \pm 0.39)\%$ and $B(\tau \to \mu\nu\bar{\nu}) = (17.02 \pm 0.31)\%$. The ratio of the muon and electron couplings to the weak charged current is measured to be $g_\mu/g_e = 1.000 \pm 0.013$, satisfying e-$\mu$ universality. The average leptonic branching fraction corrected to the value for a massless lepton, assuming e-μ universality, is found to be $B(\tau \to l\nu\bar{\nu}) = (17.50 \pm 0.25)\%$.

(To be submitted to Physics Letters B)

P.Abreu[21], W.Adam[50], T.Adye[37], E.Agasi[31], I.Ajinenko[42], R.Aleksan[39], G.D.Alekseev[16], P.P.Allport[22], S.Almehed[24], S.J.Alvsvaag[4], U.Amaldi[9], S.Amato[47], A.Andreazza[28], M.L.Andrieux[14], P.Antilogus[25], W-D.Apel[17], Y.Arnoud[39], B.Åsman[44], J-E.Augustin[19], A.Augustinus[31], P.Baillon[9], P.Bambade[19], F.Barao[21], R.Barate[14], D.Y.Bardin[16], G.J.Barker[35], A.Baroncelli[40], O.Barring[24], J.A.Barrio[26], W.Bartl[50], M.J.Bates[37], M.Battaglia[15], M.Baubillier[23], J.Baudot[39], K-H.Becks[52], M.Begalli[6], P.Beilliere[8], Yu.Belokopytov[9], A.C.Benvenuti[5], M.Berggren[47], D.Bertrand[2], F.Bianchi[45], M.Bigi[45], M.S.Bilenky[16], P.Billoir[23], D.Bloch[10], M.Blume[52], S.Blyth[35], V.Bocci[38], T.Bolognese[39], M.Bonesini[28], W.Bonivento[28], P.S.L.Booth[22], G.Borisov[42], C.Bosio[40], S.Bosworth[35], O.Botner[48], E.Boudinov[42], B.Bouquet[19], C.Bourdarios[9], T.J.V.Bowcock[22], M.Bozzo[13], P.Branchini[40], K.D.Brand[36], T.Brenke[52], R.A.Brenner[15], C.Bricman[2], L.Brillault[23], R.C.A.Brown[9], P.Bruckman[18], J-M.Brunet[8], L.Bugge[33], T.Buran[33], T.Burgsmueller[52], P.Buschmann[52], A.Buys[9], M.Caccia[28], M.Calvi[28], A.J.Camacho Rozas[41], T.Camporesi[9], V.Canale[38], M.Canepa[13], K.Cankocak[44], F.Cao[2], F.Carena[9], P.Carrilho[47], L.Carroll[22], C.Caso[13], M.V.Castillo Gimenez[49], A.Cattai[9], F.R.Cavallo[5], L.Cerrito[38], V.Chabaud[9], M.Chapkin[42], Ph.Charpentier[9], L.Chaussard[25], J.Chauveau[23], P.Checchia[36], G.A.Chelkov[16], R.Chierici[45], P.Chliapnikov[42], P.Chochula[7], V.Chorowicz[9], V.Cindro[43], P.Collins[9], J.L.Contreras[19], R.Contri[13], E.Cortina[49], G.Cosme[19], F.Cossutti[46], H.B.Crawley[1], D.Crennell[37], G.Crosetti[13], J.Cuevas Maestro[34], S.Czellar[15], E.Dahl-Jensen[29], J.Dahm[52], B.Dalmagne[19], M.Dam[33], G.Damgaard[29], A.Daum[17], P.D.Dauncey[37], M.Davenport[9], W.Da Silva[23], C.Defoix[8], G.Della Ricca[46], P.Delpierre[27], N.Demaria[35], A.De Angelis[9], H.De Boeck[2], W.De Boer[17], S.De Brabandere[2], C.De Clercq[2], C.De La Vaissiere[23], B.De Lotto[46], A.De Min[28], L.De Paula[47], C.De Saint-Jean[39], H.Dijkstra[9], L.Di Ciaccio[38], F.Djama[10], J.Dolbeau[8], M.Donszelmann[9], K.Doroba[51], M.Dracos[10], J.Drees[52], K.-A.Drees[52], M.Dris[32], Y.Dufour[8], F.Dupont[14], D.Edsall[1], R.Ehret[17], G.Eigen[4], T.Ekelof[48], G.Ekspong[44], M.Elsing[52], J-P.Engel[10], N.Ershaidat[23], B.Erzen[43], M.Espirito Santo[21], E.Falk[24], D.Fassouliotis[32], M.Feindt[9], A.Ferrer[49], T.A.Filippas[32], A.Firestone[1], P.-A.Fischer[10], H.Foeth[9], E.Fokitis[32], F.Fontanelli[13], F.Formenti[9], B.Franek[37], P.Frenkiel[8], D.C.Fries[17], A.G.Frodesen[4], R.Fruhwirth[50], F.Fulda-Quenzer[19], J.Fuster[49], A.Galloni[22], D.Gamba[45], M.Gandelman[6], C.Garcia[49], J.Garcia[41], C.Gaspar[9], U.Gasparini[36], Ph.Gavillet[9], E.N.Gazis[32], D.Gele[10], J-P.Gerber[10], M.Gibbs[22], R.Gokieli[51], B.Golob[43], G.Gopal[37], L.Gorn[1], M.Gorski[51], Yu.Gouz[42], V.Gracco[13], E.Graziani[40], G.Grosdidier[19], P.Gunnarsson[44], M.Gunther[48], J.Guy[37], U.Haedinger[17], F.Hahn[9], M.Hahn[17], S.Hahn[52], A.Hallgren[48], K.Hamacher[52], W.Hao[31], F.J.Harris[35], V.Hedberg[24], R.Henriques[21], J.J.Hernandez[49], P.Herquet[2], H.Herr[9], T.L.Hessing[9], E.Higon[49], H.J.Hilke[9], T.S.Hill[1], S-O.Holmgren[44], P.J.Holt[35], D.Holthuizen[31], M.Houlden[22], J.Hrubec[50], K.Huet[2], K.Hultqvist[44], P.Ioannou[3], J.N.Jackson[22], R.Jacobsson[44], P.Jalocha[18], R.Janik[7], G.Jarlskog[24], P.Jarry[39], B.Jean-Marie[19], E.K.Johansson[44], L.Jonsson[24], P.Jonsson[24], C.Joram[9], P.Juillot[10], M.Kaiser[17], F.Kapusta[23], M.Karlsson[44], E.Karvelas[11], S.Katsanevas[3], E.C.Katsoufis[32], R.Keranen[15], B.A.Khomenko[16], N.N.Khovanski[16], B.King[22], N.J.Kjaer[29], H.Klein[9], A.Klovning[4], P.Kluit[31], J.H.Koehne[17], B.Koene[31], P.Kokkinias[11], M.Koratzinos[9], K.Korcyl[18], V.Kostioukhine[42], C.Kourkoumelis[3], O.Kouznetsov[13], P.-H.Kramer[52], C.Kreuter[17], J.Krolikowski[51], I.Kronkvist[24], Z.Krumstein[16], W.Krupinski[18], P.Kubinec[7], W.Kucewicz[18], K.Kurvinen[15], C.Lacasta[49], I.Laktineh[25], S.Lamblot[23], J.W.Lamsa[1], L.Lanceri[46], D.W.Lane[1], P.Langefeld[52], V.Lapin[42], I.Last[22], J-P.Laugier[39], R.Lauhakangas[15], G.Leder[50], F.Ledroit[14], V.Lefebure[2], C.K.Legan[1], R.Leitner[30], Y.Lemoigne[39], J.Lemonne[2], G.Lenzen[52], V.Lepeltier[19], T.Lesiak[36], D.Liko[50], R.Lindner[52], A.Lipniacka[19], I.Lippi[36], B.Loerstad[24], M.Lokajicek[12], J.G.Loken[35], J.M.Lopez[41], A.Lopez-Fernandez[9], M.A.Lopez Aguera[41], D.Loukas[11], P.Lutz[39], L.Lyons[35], J.MacNaughton[50], G.Maehlum[17], A.Maio[21], V.Malychev[16], F.Mandl[50], J.Marco[41], B.Marechal[47], M.Margoni[36], J-C.Marin[9], C.Mariotti[40], A.Markou[11], T.Maron[52], C.Martinez-Rivero[41], F.Martinez-Vidal[49], S.Marti i Garcia[49], F.Matorras[41], C.Matteuzzi[28], G.Matthiae[38], M.Mazzucato[36], M.Mc Cubbin[9], R.Mc Kay[1], R.Mc Nulty[22], J.Medbo[48], C.Meroni[28], W.T.Meyer[1], M.Michelotto[36], E.Migliore[45], L.Mirabito[25], W.A.Mitaroff[50], U.Mjoernmark[24], T.Moa[44], R.Moeller[29], K.Moenig[9], M.R.Monge[13], P.Morettini[13], H.Mueller[17], L.M.Mundim[6], W.J.Murray[37], B.Muryn[18], G.Myatt[35], F.Naraghi[14], F.L.Navarria[5], S.Navas[49], P.Negri[28], S.Nemecek[12], W.Neumann[52], N.Neumeister[50], R.Nicolaidou[3], B.S.Nielsen[29], M.Nieuwenhuizen[31], V.Nikolaenko[10], P.Niss[44], A.Nomerotski[36], A.Normand[35], W.Oberschulte-Beckmann[17], V.Obraztsov[42], A.G.Olshevski[16], A.Onofre[21], R.Orava[15], K.Osterberg[15], A.Ouraou[39], P.Paganini[19], M.Paganoni[28], P.Pages[10], H.Palka[18], Th.D.Papadopoulou[32], L.Pape[9], C.Parkes[35], F.Parodi[13], A.Passeri[40], M.Pegoraro[36], L.Peralta[21], H.Pernegger[50], M.Pernicka[50], A.Perrotta[5], C.Petridou[46], A.Petrolini[13], H.T.Phillips[37], G.Piana[13], F.Pierre[39], M.Pimenta[21], S.Plaszczynski[19], O.Podobrin[17], M.E.Pol[6], G.Polok[18], P.Poropat[46], V.Pozdniakov[16], M.Prest[46], P.Privitera[38], N.Pukhaeva[16], A.Pullia[28], D.Radojicic[35], S.Ragazzi[28], H.Rahmani[32], J.Rames[12], P.N.Ratoff[20], A.L.Read[33], M.Reale[52], P.Rebecchi[19], N.G.Redaelli[28], M.Regler[50], D.Reid[9], P.B.Renton[35], L.K.Resvanis[3], F.Richard[19], J.Richardson[22], J.Ridky[12], G.Rinaudo[45], I.Ripp[39], A.Romero[45], I.Roncagliolo[13], P.Ronchese[36], L.Roos[14], E.I.Rosenberg[1], E.Rosso[9], P.Roudeau[19], T.Rovelli[5], W.Ruckstuhl[31], V.Ruhlmann-Kleider[39], A.Ruiz[41], H.Saarikko[15], Y.Sacquin[39], A.Sadovsky[16], G.Sajot[14], J.Salt[49], J.Sanchez[26], M.Sannino[13], H.Schneider[17], M.A.E.Schyns[52], G.Sciolla[45], F.Scuri[46], Y.Sedykh[16], A.M.Segar[35], A.Seitz[17], R.Sekulin[37], R.C.Shellard[6], I.Siccama[31], P.Siegrist[39], S.Simonetti[39], F.Simonetto[36], A.N.Sisakian[16], B.Sitar[7], T.B.Skaali[33], G.Smadja[25], N.Smirnov[42], O.Smirnova[16], G.R.Smith[37], R.Sosnowski[51], D.Souza-Santos[6], T.Spassov[21], E.Spiriti[40], P.Sponholz[52], S.Squarcia[13], C.Stanescu[40], S.Stapnes[33], I.Stavitski[36], K.Stepaniak[51], F.Stichelbaut[9], A.Stocchi[19], J.Strauss[50], R.Strub[10], B.Stugu[4], M.Szczekowski[51], M.Szeptycka[51], T.Tabarelli[28], J.P.Tavernet[23], O.Tchikilev[42], A.Tilquin[27], J.Timmermans[31], L.G.Tkatchev[16], T.Todorov[10], D.Z.Toet[31], A.Tomaradze[2], B.Tome[21], L.Tortora[40], G.Transtromer[24], D.Treille[9],

W.Trischuk[9], G.Tristram[8], A.Trombini[19], C.Troncon[28], A.Tsirou[9], M-L.Turluer[39], I.A.Tyapkin[16], M.Tyndel[37], S.Tzamarias[22], B.Ueberschaer[52], O.Ullaland[9], V.Uvarov[42], G.Valenti[5], E.Vallazza[9], C.Vander Velde[2], G.W.Van Apeldoorn[31], P.Van Dam[31], W.K.Van Doninck[2], J.Van Eldik[31], N.Vassilopoulos[35], G.Vegni[28], L.Ventura[36], W.Venus[37], F.Verbeure[2], M.Verlato[36], L.S.Vertogradov[16], D.Vilanova[39], P.Vincent[25], L.Vitale[46], E.Vlasov[42], A.S.Vodopyanov[16], V.Vrba[12], H.Wahlen[52], C.Walck[44], F.Waldner[46], M.Weierstall[52], P.Weilhammer[9], A.M.Wetherell[9], D.Wicke[52], J.H.Wickens[2], M.Wielers[17], G.R.Wilkinson[35], W.S.C.Williams[35], M.Winter[10], M.Witek[9], K.Woschnagg[48], K.Yip[35], O.Yushchenko[42], F.Zach[25], C.Zacharatou[24], A.Zaitsev[42], A.Zalewska[18], P.Zalewski[51], D.Zavrtanik[43], E.Zevgolatakos[11], N.I.Zimin[16], M.Zito[39], D.Zontar[43], R.Zuberi[35], G.C.Zucchelli[44], G.Zumerle[36]

[1] Ames Laboratory and Department of Physics, Iowa State University, Ames IA 50011, USA
[2] Physics Department, Univ. Instelling Antwerpen, Universiteitsplein 1, B-2610 Wilrijk, Belgium
and IIHE, ULB-VUB, Pleinlaan 2, B-1050 Brussels, Belgium
and Faculté des Sciences, Univ. de l'Etat Mons, Av. Maistriau 19, B-7000 Mons, Belgium
[3] Physics Laboratory, University of Athens, Solonos Str. 104, GR-10680 Athens, Greece
[4] Department of Physics, University of Bergen, Allégaten 55, N-5007 Bergen, Norway
[5] Dipartimento di Fisica, Università di Bologna and INFN, Via Irnerio 46, I-40126 Bologna, Italy
[6] Centro Brasileiro de Pesquisas Físicas, rua Xavier Sigaud 150, RJ-22290 Rio de Janeiro, Brazil
and Depto. de Física, Pont. Univ. Católica, C.P. 38071 RJ-22453 Rio de Janeiro, Brazil
and Inst. de Física, Univ. Estadual do Rio de Janeiro, rua São Francisco Xavier 524, Rio de Janeiro, Brazil
[7] Comenius University, Faculty of Mathematics and Physics, Mlynska Dolina, SK-84215 Bratislava, Slovakia
[8] Collège de France, Lab. de Physique Corpusculaire, IN2P3-CNRS, F-75231 Paris Cedex 05, France
[9] CERN, CH-1211 Geneva 23, Switzerland
[10] Centre de Recherche Nucléaire, IN2P3 - CNRS/ULP - BP20, F-67037 Strasbourg Cedex, France
[11] Institute of Nuclear Physics, N.C.S.R. Demokritos, P.O. Box 60228, GR-15310 Athens, Greece
[12] FZU, Inst. of Physics of the C.A.S. High Energy Physics Division, Na Slovance 2, 180 40, Praha 8, Czech Republic
[13] Dipartimento di Fisica, Università di Genova and INFN, Via Dodecaneso 33, I-16146 Genova, Italy
[14] Institut des Sciences Nucléaires, IN2P3-CNRS, Université de Grenoble 1, F-38026 Grenoble Cedex, France
[15] Research Institute for High Energy Physics, SEFT, P.O. Box 9, FIN-00014 Helsinki, Finland
[16] Joint Institute for Nuclear Research, Dubna, Head Post Office, P.O. Box 79, 101 000 Moscow, Russian Federation
[17] Institut für Experimentelle Kernphysik, Universität Karlsruhe, Postfach 6980, D-76128 Karlsruhe, Germany
[18] High Energy Physics Laboratory, Institute of Nuclear Physics, Ul. Kawiory 26a, PL-30055 Krakow 30, Poland
[19] Université de Paris-Sud, Lab. de l'Accélérateur Linéaire, IN2P3-CNRS, Bât. 200, F-91405 Orsay Cedex, France
[20] School of Physics and Materials, University of Lancaster, Lancaster LA1 4YB, UK
[21] LIP, IST, FCUL - Av. Elias Garcia, 14-1^{o}, P-1000 Lisboa Codex, Portugal
[22] Department of Physics, University of Liverpool, P.O. Box 147, Liverpool L69 3BX, UK
[23] LPNHE, IN2P3-CNRS, Universités Paris VI et VII, Tour 33 (RdC), 4 place Jussieu, F-75252 Paris Cedex 05, France
[24] Department of Physics, University of Lund, Sölvegatan 14, S-22363 Lund, Sweden
[25] Université Claude Bernard de Lyon, IPNL, IN2P3-CNRS, F-69622 Villeurbanne Cedex, France
[26] Universidad Complutense, Avda. Complutense s/n, E-28040 Madrid, Spain
[27] Univ. d'Aix - Marseille II - CPP, IN2P3-CNRS, F-13288 Marseille Cedex 09, France
[28] Dipartimento di Fisica, Università di Milano and INFN, Via Celoria 16, I-20133 Milan, Italy
[29] Niels Bohr Institute, Blegdamsvej 17, DK-2100 Copenhagen 0, Denmark
[30] NC, Nuclear Centre of MFF, Charles University, Areal MFF, V Holesovickach 2, 180 00, Praha 8, Czech Republic
[31] NIKHEF-H, Postbus 41882, NL-1009 DB Amsterdam, The Netherlands
[32] National Technical University, Physics Department, Zografou Campus, GR-15773 Athens, Greece
[33] Physics Department, University of Oslo, Blindern, N-1000 Oslo 3, Norway
[34] Dpto. Fisica, Univ. Oviedo, C/P. Pérez Casas, S/N-33006 Oviedo, Spain
[35] Department of Physics, University of Oxford, Keble Road, Oxford OX1 3RH, UK
[36] Dipartimento di Fisica, Università di Padova and INFN, Via Marzolo 8, I-35131 Padua, Italy
[37] Rutherford Appleton Laboratory, Chilton, Didcot OX11 OQX, UK
[38] Dipartimento di Fisica, Università di Roma II and INFN, Tor Vergata, I-00173 Rome, Italy
[39] Centre d'Etudes de Saclay, DSM/DAPNIA, F-91191 Gif-sur-Yvette Cedex, France
[40] Istituto Superiore di Sanità, Ist. Naz. di Fisica Nucl. (INFN), Viale Regina Elena 299, I-00161 Rome, Italy
[41] C.E.A.F.M., C.S.I.C. - Univ. Cantabria, Avda. los Castros, S/N-39006 Santander, Spain, (CICYT-AEN93-0832)
[42] Inst. for High Energy Physics, Serpukov P.O. Box 35, Protvino, (Moscow Region), Russian Federation
[43] J. Stefan Institute and Department of Physics, University of Ljubljana, Jamova 39, SI-61000 Ljubljana, Slovenia
[44] Fysikum, Stockholm University, Box 6730, S-113 85 Stockholm, Sweden
[45] Dipartimento di Fisica Sperimentale, Università di Torino and INFN, Via P. Giuria 1, I-10125 Turin, Italy
[46] Dipartimento di Fisica, Università di Trieste and INFN, Via A. Valerio 2, I-34127 Trieste, Italy
and Istituto di Fisica, Università di Udine, I-33100 Udine, Italy
[47] Univ. Federal do Rio de Janeiro, C.P. 68528 Cidade Univ., Ilha do Fundão BR-21945-970 Rio de Janeiro, Brazil
[48] Department of Radiation Sciences, University of Uppsala, P.O. Box 535, S-751 21 Uppsala, Sweden
[49] IFIC, Valencia-CSIC, and D.F.A.M.N., U. de Valencia, Avda. Dr. Moliner 50, E-46100 Burjassot (Valencia), Spain
[50] Institut für Hochenergiephysik, Österr. Akad. d. Wissensch., Nikolsdorfergasse 18, A-1050 Vienna, Austria
[51] Inst. Nuclear Studies and University of Warsaw, Ul. Hoza 69, PL-00681 Warsaw, Poland
[52] Fachbereich Physik, University of Wuppertal, Postfach 100 127, D-42097 Wuppertal 1, Germany

1 Introduction

The LEP collider at CERN, in which e^+e^- collisions take place at centre-of-mass energies $\sqrt{s} \simeq 91$ GeV, produces τ lepton pairs through the reaction $e^+e^- \to Z^0 \to \tau^+\tau^-$. The branching fractions of the decays $\tau \to \mu\nu\bar{\nu}$ and $\tau \to e\nu\bar{\nu}$ can be used to test universality in the couplings of the leptons to the weak charged current. Assuming the neutrino to be massless, the ratio of the widths for the decays into leptonic final states is given by [1]

$$\frac{\Gamma(\tau \to \mu\nu\bar{\nu})}{\Gamma(\tau \to e\nu\bar{\nu})} = \frac{g_\mu^2}{g_e^2} \cdot \frac{f(M_\mu^2/M_\tau^2)}{f(M_e^2/M_\tau^2)}, \tag{1}$$

where g_μ and g_e are the couplings of the muon and electron to the charged weak current, M_μ and M_e are their masses, M_τ is the mass of the τ, and

$$f(x) = 1 - 8x + 8x^3 - x^4 - 12x^2 \ln x. \tag{2}$$

The function $f(x)$ is a phase space suppression factor and has the values 1.000 and 0.973 for the electron and muon respectively, using the world average values for the masses of the charged leptons [2].

2 Method

The selection of leptonic τ decays proceeded in three stages. Firstly, an initial sample of $\tau^+\tau^-$ events was selected. Then channel dependent selections of τ decays were made in order to reduce the level of backgrounds from non-τ sources: each τ decay was considered for lepton identification if the opposing τ decay satisfied specific requirements. Leptonic decays were then identified from these τ decay samples.

The branching fraction for the decay of the τ to lepton l was measured using the expression

$$B(\tau \to l\nu\bar{\nu}) = \frac{N_l}{N_\tau} \cdot \frac{1 - b_l}{1 - b_\tau} \cdot \frac{1}{\epsilon_l c_l}, \tag{3}$$

where N_l is the number of identified leptonic decays, ϵ_l is the lepton identification efficiency after the τ decay selection cuts have been applied, b_l is the background fraction in the lepton sample, N_τ is the number of τ decays in the final sample, b_τ is the background fraction in the τ decay sample, and the bias factor c_l is the ratio of the τ decay selection efficiency for the decay channel $\tau \to l\nu\bar{\nu}$ to the overall τ decay selection efficiency.

The performance of the procedures used to select $\tau \to e\nu\bar{\nu}$ and $\tau \to \mu\nu\bar{\nu}$ decays was studied using simulated data and test samples identified in the data from kinematic constraints. The redundancy between different components of the detector allowed detailed studies of the detector response.

3 The DELPHI detector

The DELPHI detector and its performance is described in detail elsewhere [3]. In the DELPHI reference frame the z-axis is along the direction of the electron beam, θ is the polar angle with respect to the z-axis, and ϕ is the azimuthal angle about this axis. The lepton identification was confined to the barrel part of the detector, satisfying the condition $|\cos\theta| < 0.731$. The relevant sub-detector elements are described here.

Charged particle trajectories were reconstructed in the barrel region using four cylindrical tracking detectors in a 1.2 Tesla magnetic field parallel to the beam direction. The Vertex Detector (VD) consisted of three layers of silicon microstrip modules at radii, R, between 6.3 and 11.0 cm from the beam axis. Situated between R of 12 cm and 28 cm was the Inner Detector (ID), a jet chamber which provided 24 $R\Phi$ coordinates. The principal tracking device was the Time Projection Chamber (TPC), which extended from 30 to 122 cm in radius, and gave up to 16 space points for pattern recognition. Small regions of reduced tracking efficiency occurred every 60° in ϕ, the boundaries between sectors, and between the two halves along the z-axis, at $\theta = 90°$. The measurement of charged particle energy loss through ionisation, dE/dx, from 192 anode sense wires allowed the separation of electrons from more massive particles, especially below momenta of 15 GeV/c. The momentum threshold for the separation of electrons from pions was around 0.4 GeV/c, and the dE/dx resolution for isolated tracks in τ decays was 6.1%. Finally, the Outer Detector (OD), which consisted of five layers of drift cells, was situated at a radius of two metres from the beam axis. The precision on the momentum component transverse to the beam direction, p_t, using the tracking detectors was $\Delta(1/p_t) = 0.0008$ $(\mathrm{GeV/c})^{-1}$ for muons in non-radiative $\mathrm{Z}^0 \to \mu^+\mu^-$ events.

Particle identification in this analysis relied on the following sub-detector elements. The High density Projection Chamber (HPC) was an electromagnetic calorimeter 18 radiation lengths deep, with an energy resolution of $(32\%/\sqrt{E(\mathrm{GeV})}) \oplus 4.4\%$. Its high granularity and sampling of shower energies from nine layers in depth allowed an accurate determination of the position of the start of the shower. Every 15° in azimuth, and at $\theta = 90°$, there were inter-module boundaries which led to a poorer energy resolution for electromagnetic showers. The Hadron Calorimeter (HCAL) consisted of 110 cm of iron segmented into four layers in depth, and was sensitive to hadronic showers and minimum ionising particles. The barrel Muon Chambers (MUB) comprised two layers of drift tubes after 90 and 110 cm of iron. The polar angle acceptance was $|\cos\theta| < 0.602$, which was smaller than the other barrel detectors. The range $|\cos\theta| > 0.602$ was covered by the forward Muon Chambers in certain azimuthal regions.

A further restriction in the polar angle acceptance of the lepton identification ($0.035 < |\cos\theta|$) was introduced due to the reduced tracking efficiency of the TPC and the poorer energy resolution of the HPC at $\theta = 90°$.

4 Initial $\tau^+\tau^-$ selection

The decay $\mathrm{Z}^0 \to \tau^+\tau^-$ at LEP energies is characterised by two low multiplicity, highly collimated, back-to-back jets of particles, with significant missing energy due to the undetected neutrinos from the τ decays. The $\tau^+\tau^-$ event selection described here was common to both leptonic decay channels; details can be found in [4].

Each event was divided into hemispheres by a plane perpendicular to the thrust axis, which was calculated using the charged particles. Both hemispheres had to contain at least one charged particle. The highest momentum charged particle in each hemisphere was defined as the leading particle for that hemisphere. At least one of the two leading particles per event was required to lie in the barrel region of the detector.

The points of closest approach of the leading particles from the centre of the interaction region had to be less than 1.5 cm in the $R\Phi$ plane and less than 4.5 cm in z. These cuts removed most of the background from cosmic rays.

The background from hadronic decays of the Z^0 was reduced by asking for a maximum of six charged particles originating from the interaction region. The isolation angle,

defined as the minimum angle between any two charged particles in different hemispheres, had to be greater than 160°.

Two-photon events were rejected by requiring that the total energy in the event, E_{vis}, defined as the sum of the neutral electromagnetic energy and the energy of the charged particles, be greater than 8 GeV, and by demanding that the total transverse momentum, with respect to the beam axis, of the charged particles in the event be greater than 0.4 GeV/c.

Most of the decays $Z^0 \to \mu^+\mu^-$ and $Z^0 \to e^+e^-$ were excluded by requiring that the acollinearity between the leading charged particles be greater than 0.5°, the variable $p_{rad} = \sqrt{p_1^2 + p_2^2}$ be less than the beam momentum p_{beam}, and $E_{rad} = \sqrt{E_1^2 + E_2^2}$ be less than the beam energy E_{beam}. The variables p_1, p_2 are the momenta of the leading particles, and E_1, E_2 are the electromagnetic energies deposited in a cone of half-angle 30° around these particles.

By comparing the response of independent components, the trigger efficiency was found to be $(99.98 \pm 0.01)\%$ for $\tau^+\tau^-$ final states. Using these cuts, around 25000 $Z^0 \to \tau^+\tau^-$ events were selected from 1991 and 1992 data. The efficiency from simulation was $(82.0 \pm 0.5)\%$ within the angular acceptance. The total background, also determined from simulation, was $(2.8 \pm 0.4)\%$, of which $(1.8 \pm 0.3)\%$ came from $Z^0 \to e^+e^-$ and $e^+e^- \to (e^+e^-)e^+e^-$ events, $(0.5 \pm 0.1)\%$ was from $Z^0 \to \mu^+\mu^-$ and $e^+e^- \to (e^+e^-)\mu^+\mu^-$ events, and $(0.5 \pm 0.2)\%$ from $Z^0 \to q\bar{q}$ events. The error on the efficiency had little effect on the final branching fraction results.

5 Analysis of $\tau \to e\nu\bar{\nu}$ decays

5.1 Further τ decay selection

The leading particle in each hemisphere was required to be within the polar angle acceptance of the TPC and HPC ($0.035 < |\cos\theta| < 0.731$), to optimise the rejection of background from $Z^0 \to e^+e^-$ events. It was then required that the total deposited electromagnetic energy in the hemisphere opposite the τ decay considered for identification be less than $0.8 \times E_{beam}$. In the regions close to the boundaries between HPC modules the energy deposited in the first layer of the HCAL was included in this energy sum. Electron backgrounds from $e^+e^- \to (e^+e^-)e^+e^-$ interactions were effectively reduced by requiring that the measured dE/dx for the track in the opposite hemisphere be inconsistent with the value expected for an electron, in events with only two charged particles, both with momentum less than $0.2 \times p_{beam}$.

The performance of the electron identification was enhanced by requiring that the leading particles extrapolated to a point on the HPC surface more than 1° away from the centre of an azimuthal inter-module boundary. Furthermore, the ionisation in the TPC had to be recorded by a minimum of 38 anode sense wires. This led to a 4.1% loss of tracks around the boundary regions between the six azimuthal TPC sectors, which was well described by simulation.

The details of the selected τ decay sample are listed in Table 1. There were 31325 τ decays selected, with a background fraction, b_τ, of 0.013 ± 0.004. The criteria used to select this sample led to a bias factor $c_e = 0.993 \pm 0.012$, determined from simulation. The error on c_e was obtained from comparisons between real and simulated data. The major contribution to the uncertainty resulted from the loss of tracks close to the boundaries between TPC sectors, which was slightly larger for electrons than for other particles. The uncertainty was estimated from the stability of the identified electron fraction when the

problematic regions were excluded, and from a separate study of badly measured tracks; it was found to be ± 0.010. Other uncertainties were estimated by propagating the errors on the variables used to define the τ decay sample. The significant errors came from the variables E_{vis}, E_{rad} and p_{rad}, and led to an error of ± 0.004 on c_e.

	$\tau \to e\nu\bar{\nu}$	$\tau \to \mu\nu\bar{\nu}$
N_τ	31325	41122
c_l	0.993 ± 0.012	1.077 ± 0.008
b_τ	0.013 ± 0.004	0.019 ± 0.006
N_l	5059	6586
ϵ_l	0.909 ± 0.009	0.855 ± 0.008
b_l: total	0.035 ± 0.009	0.039 ± 0.005
$\tau \to$ hadrons	0.022 ± 0.005	0.032 ± 0.004
non-τ	0.013 ± 0.007	0.007 ± 0.002

Table 1: Number of decays, efficiencies and background fractions for the decay channels $\tau \to e\nu\bar{\nu}$ and $\tau \to \mu\nu\bar{\nu}$. The variables are explained in Section 2.

5.2 Electron identification

The main variables used for electron identification were the dE/dx measurement in the TPC, and the ratio of the associated electromagnetic energy deposited in the HPC and the particle momentum, E/p. For both of these quantities pull variables were constructed which were based on the measured value of the variable, its resolution and the value expected for a given particle type. The variables $\Pi^e_{dE/dx}$ and $\Pi_{E/p}$ are defined as the signed number of standard deviations by which the measured value differed from the expectation for an electron; a similar variable based on the pion hypothesis $\Pi^\pi_{dE/dx}$ was also used.

For a particle to be identified as an electron it had to be the only charged particle in the hemisphere, and have a momentum greater than $0.01 \times p_{beam}$. Losses due to electrons showering before the TPC were studied using real and simulated data test samples, and were found to be $(2.5 \pm 0.5)\%$. The dE/dx was first required to be compatible with the expectation for an electron by demanding that $\Pi^e_{dE/dx}$ be greater than -2. This reduced the background from hadrons and muons, especially at low momenta, with little effect on the signal. Then a high identification efficiency over the whole momentum range was ensured by a logical "or" of criteria based on dE/dx and E/p: for particles with momentum greater than $0.05 \times p_{beam}$ it was required that $\Pi_{E/p}$ be greater than -2, while for particles with momentum less than $0.5 \times p_{beam}$ it was required that $\Pi^\pi_{dE/dx}$ be greater than 3.

The residual backgrounds from hadronic τ decays were reduced by vetoing decays with energy deposited beyond the first layer of the HCAL. It was also required that there be no neutral electromagnetic shower with an energy greater than 4 GeV inside a cone of half-angle 18° around the particle. Showers originating from neutral particles within 1° in polar angle of the track, which appeared to originate from bremsstrahlung, were excluded from this requirement.

The identification efficiency from simulation was checked at high energies using $Z^0 \to e^+e^-$ events, and at low energies with a high purity sample of $e^+e^- \to (e^+e^-)e^+e^-$ events.

The redundancy between dE/dx and E/p at intermediate energies enabled precise studies of the efficiency of these two variables. The electron identification efficiency after the τ decay selection, ϵ_l, was $(90.9 \pm 0.9)\%$. The main contributions to the error came from the requirement that there be a single charged particle in the hemisphere ($\pm 0.6\%$), the "or" of the dE/dx and E/p requirements ($\pm 0.4\%$), and the neutral veto ($\pm 0.5\%$).

The misidentification probability for hadrons obtained from simulation was similarly checked by exploiting the dE/dx versus calorimeter redundancy. In addition, a test sample of hadrons from $\tau \to \rho\nu$ and $\tau \to \mathrm{a_1}\nu$ decays, selected by tagging π^0's in the HPC, was used to correct the background estimation from simulation. A discrepancy was found in the response of the HPC to hadrons between real and simulated data, leading to a correction and systematic error for the background estimate from simulation. Figures 1 and 2 show the variables $\Pi^e_{dE/dx}$ and $\Pi_{E/p}$ for various samples of charged particles. The background from $\mathrm{e^+e^-} \to (\mathrm{e^+e^-})\mathrm{e^+e^-}$ interactions was found to be well described by the simulation. Studies of events with identified electrons in both hemispheres showed that a correction was needed for the estimate of the background from $\mathrm{Z^0} \to \mathrm{e^+e^-}$ events from simulation. The background fraction for the $\tau \to e\nu\bar{\nu}$ decay sample, b_l, was found to be 0.035 ± 0.009.

There were 5059 $\tau \to e\nu\bar{\nu}$ decays identified. The identification efficiency and backgrounds are summarised in Table 1. The contribution to the background from $\tau \to \mu\nu\bar{\nu}$ decays was negligible.

6 Analysis of $\tau \to \mu\nu\bar{\nu}$ decays

6.1 Further τ decay selection

For the purposes of reducing the backgrounds from non-τ sources, and then to identify muons, a loose muon candidate was defined as a particle with associated hits in the muon chambers or energy deposited in the outer layer of the HCAL.

The background from $\mathrm{Z^0} \to \mu^+\mu^-$ events was reduced by criteria based on the existance of a loose muon candidate in the hemisphere opposite the particle considered for identification. If such a loose muon candidate existed, it was required that its momentum be less than $0.7 \times p_{beam}$, and the momentum of the particle to be identified be less than $0.8 \times p_{beam}$. Backgrounds from $\mathrm{e^+e^-} \to (\mathrm{e^+e^-})\mu^+\mu^-$ interactions were suppressed by requiring, in the case of a loose muon candidate in the opposite hemisphere, at least one particle in the event with momentum greater than 9 GeV/c. The cosmic ray background was decreased by tightening the vertex cuts described in Section 4, requiring that at least one of the two leading particles in the event had a perigee with respect to the centre of the interaction region of less than 0.3 cm in the $R\Phi$ plane.

The particle to be identified was required to be within the polar angle acceptance of the TPC, HCAL and muon chambers ($0.035 < |\cos\theta| < 0.731$).

The details of the final τ decay sample for the $\tau \to \mu\nu\bar{\nu}$ analysis are shown in Table 1. There were 41122 τ decays selected, with a background fraction, b_τ, of 0.019 ± 0.006. The criteria used to select this sample led to a bias factor $c_\mu = 1.077 \pm 0.008$, determined from simulation. This relatively large bias for the muon channel came mainly from the cuts on the maximum number of charged particles in the event and on E_{rad}, used to define the τ decay sample. The error on c_μ was determined from comparisons between real and simulated data. The uncertainty from track losses was smaller than in the electron case (± 0.005). Other contributions were estimated by considering the uncertainties in scale

and resolution of the variables used to select the sample. The significant errors came from the variables E_{rad} and E_{vis}, leading to an error of ± 0.005 on c_μ.

6.2 Muon identification

For a particle to be identified as a muon, it had to satisfy the loose candidate requirements, be the only charged particle in the hemisphere, and have a momentum greater than 3 GeV/c, in order to reach the muon chambers. Rejection of τ hadronic decays penetrating deep into the HCAL was ensured by asking for the particle to be minimum ionising: the average energy deposited per active layer of the HCAL, E_{hlay}, was required to be less than 3 GeV. Figure 3 shows this variable for test samples of muons and pions. Hadronic decays of the τ in which an isolated particle was accompanied by one or more π^0's, or interacted in the HPC, were rejected by requiring a maximum neutral electromagnetic energy of 1 GeV in a cone of half-angle 18° around the particle, and a maximum electromagnetic energy associated to the particle of 3 GeV.

Test samples of $Z^0 \to \mu^+\mu^-$ and $e^+e^- \to (e^+e^-)\mu^+\mu^-$ events from data were used to check the estimates from simulation of the efficiencies in the high and low momentum regions. The efficiency of the requirement on the "or" of the muon chamber hits and the outer layer of the HCAL was the same for both these event samples, and thus was assumed to be constant over the whole momentum range. For intermediate momenta, a high purity muon sample was extracted from τ decays by strict requirements on the observed hit pattern in the MUB. From this sample the efficiency of all the identification criteria, except for the loose muon candidate requirements, was obtained. The muon identification efficiency after the τ decay selection, ϵ_l, was $(85.5 \pm 0.8)\%$. The main contributions to the error came from the requirement that there be a single charged particle in the hemisphere ($\pm 0.4\%$), and from the muon identification criteria ($\pm 0.6\%$).

The hadron misidentification probability was obtained from simulation studies and from the hadronic τ decay test sample mentioned in Section 5. The cosmic ray background was estimated by interpolating the observed density of events far from the vertex region into the region of the tight vertex cuts. Backgrounds from $Z^0 \to \mu^+\mu^-$ and $e^+e^- \to (e^+e^-)\mu^+\mu^-$ events were found to be well described by simulation. The background fraction for the $\tau \to \mu\nu\bar{\nu}$ decay sample, b_l, was found to be 0.039 ± 0.005.

There were 6586 identified $\tau \to \mu\nu\bar{\nu}$ decays. The identification efficiency and backgrounds are summarised in Table 1. The contribution to the background from $\tau \to e\nu\bar{\nu}$ decays was negligible.

7 Results and Conclusions

From the numbers listed in Table 1 the τ leptonic branching fractions were found to be

$$B(\tau \to e\nu\bar{\nu}) = (17.51 \pm 0.23_{stat} \pm 0.31_{sys})\%, \quad (4)$$

$$B(\tau \to \mu\nu\bar{\nu}) = (17.02 \pm 0.19_{stat} \pm 0.24_{sys})\%. \quad (5)$$

The contributions to the systematic errors are listed in Table 2, and are propagated from the errors on the quantities as given in Table 1. Due to the precise measurement of the τ polarisation in Z^0 decays from DELPHI [5], the uncertainty from this source was estimated to be negligible. The results are in agreement with the current world average values [2], with recent measurements by OPAL [6], and with the previously published DELPHI results based on 1990 data [7], which they supersede.

source of uncertainty	$\tau \to e\nu\bar{\nu}$	$\tau \to \mu\nu\bar{\nu}$
data statistics	0.23	0.19
$\tau^+\tau^-$ selection	0.21	0.14
identification efficiency	0.18	0.15
backgrounds from non-τ decays	0.12	0.12
backgrounds from τ decays	0.09	0.07
total systematics	0.31	0.24

Table 2: Summary of the absolute uncertainties on the leptonic branching fractions.

A test of e-μ universality in the weak charged current can be performed by calculating the ratio of the muon and electron branching fractions

$$\frac{B(\tau \to \mu\nu\bar{\nu})}{B(\tau \to e\nu\bar{\nu})} = 0.972 \pm 0.017_{stat} \pm 0.020_{sys}. \tag{6}$$

Here, the 20% correlation in the systematic errors from the τ selection and the non-τ background is taken into account. Using equations 1 and 2 this can be expressed in terms of the muon and electron couplings to the charged weak current as

$$\frac{g_\mu}{g_e} = 1.000 \pm 0.013. \tag{7}$$

Assuming e-μ universality the two branching fractions can be combined to obtain an average branching fraction to massless charged leptons

$$B(\tau \to l\nu\bar{\nu}) = (17.50 \pm 0.15_{stat} \pm 0.20_{sys})\%. \tag{8}$$

Acknowledgements

We are greatly indebted to our technical collaborators and to the funding agencies for their support in building and operating the DELPHI detector, and to the members of the CERN-SL Division for the excellent performance of the LEP collider.

References

[1] W. Marciano and A. Sirlin, Phys. Rev. Lett. **61** (1988) 1815.
[2] Particle Data Group, Phys. Rev. **D50** (1994) 1173.
[3] DELPHI Collaboration, P.Aarnio et al., Nucl. Instr. and Meth. **A303** (1991) 233.
[4] DELPHI Collaboration, P.Abreu et al., Nucl. Phys. **B417** (1994) 3.
[5] DELPHI Collaboration, P.Abreu et al., CERN preprint CERN-PPE/95-30 (1995).
[6] OPAL Collaboration, R.Akers et al., CERN preprint CERN-PPE/95-06 (1995).
[7] DELPHI Collaboration, P.Abreu et al., Z. Phys. **C55** (1992) 555.

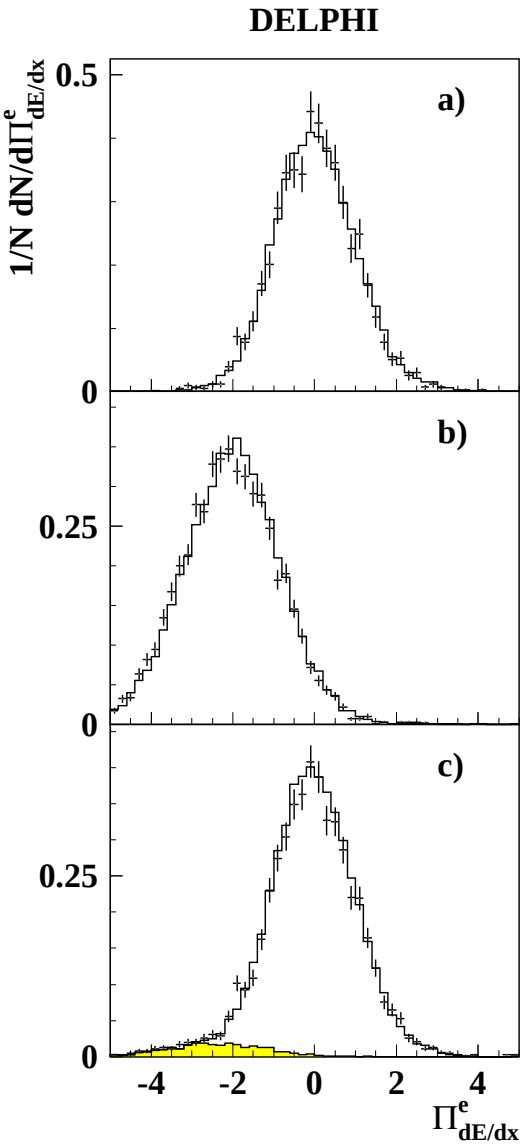

Figure 1: Distribution of the pull on dE/dx for the electron hypothesis, $\Pi^e_{dE/dx}$, for a) an electron test sample, b) a hadron test sample and c) after all other electron identification cuts. The points with error bars are real data, the unshaded histogram is simulated data, and the shaded histogram is the simulated background from τ decays.

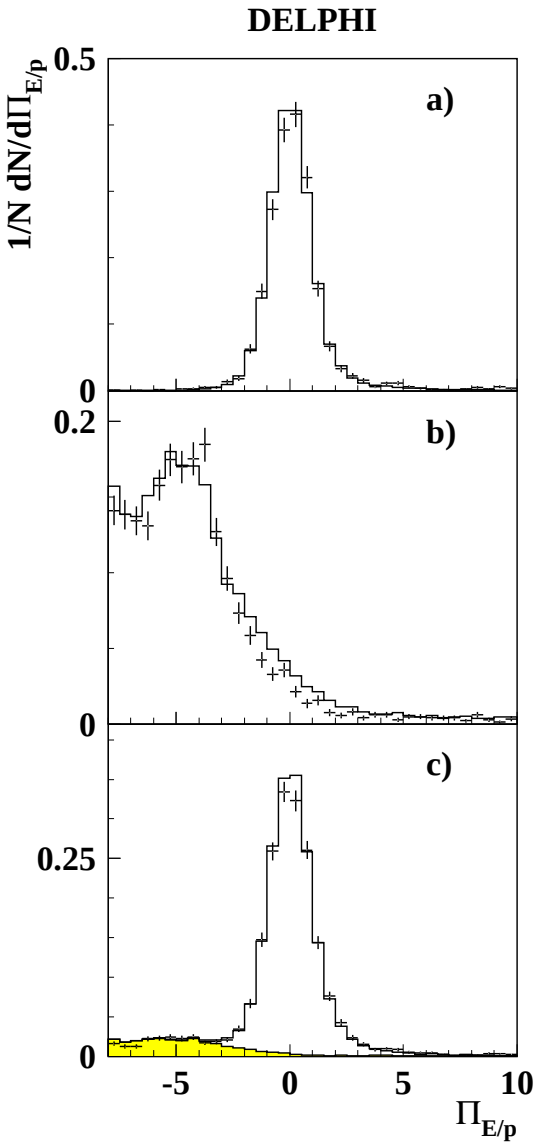

Figure 2: Distribution of the pull on E/p for the electron hypothesis, $\Pi_{E/p}$, for a) an electron test sample, b) a hadron test sample and c) after all other electron identification cuts. The points with error bars are real data, the unshaded histogram is simulated data, and the shaded histogram is the simulated background from τ decays. The discrepancy in the HPC reponse to hadrons is clearly visible.

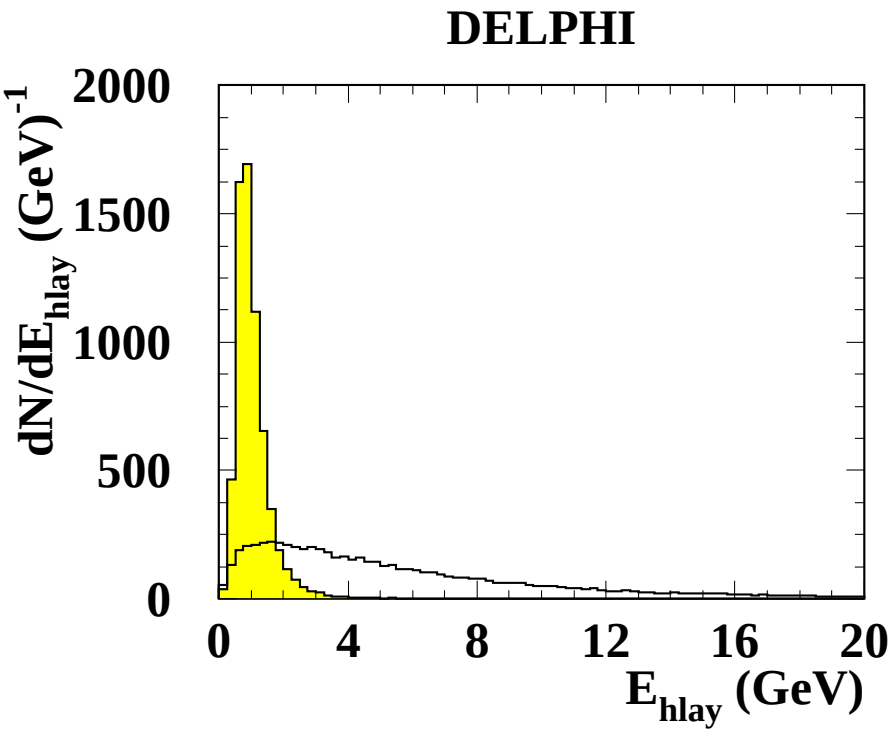

Figure 3: Distribution of the average energy per layer E_{hlay} in the hadron calorimeter for real data test samples of pions (unshaded histogram) and of muons (shaded histogram). Entries with $E_{hlay} = 0$ have been suppressed.